Macromolecular Research, Vol. 12, No. 2, pp 172-177 (2004)

Development of Lamellar Morphology in Poly(ethylene terephthalate)/Polycarbonate Blends

Jong Kwan Lee, Jeong Eun Im, and Kwang Hee Lee*

Center for Advanced Functional Polymers, School of Chemical Science and Engineering, Inha University, Inchon 402-751, Korea

Received April 17, 2003; Revised December 4, 2003

Abstract: We have studied the lamellar-level morphology of poly(ethylene terephthalate) (PET)/polycarbonate (PC) blends using small-angle X-ray scattering (SAXS). Measurements were made as a function of the holding time in the melt. We determined the morphological parameters at the lamellar level by correlation function analysis of the SAXS data. An increased amorphous layer thickness was identified in the blend, indicating that some PC was incorporated into the interlamellar regions of PET during crystallization. The blend also exhibits a larger lamellar crystalline thickness (l_c) than that of pure PET. A possible reason for the increase in l_c is that the inclusion of the PC molecules in the interlamellar regions causes an increase in the surface free energy of folding. At the early stage of isothermal crystallization, we observed a rapid drop in the value of l_c in the blend; this finding indicates that a relatively large fraction of secondary crystals form during the primary crystallization. In contrast, the value of l_c for the sample that underwent a prolonged holding time increased with time in the secondary crystallization-dominant regime; this observation suggests that the disruption of chain periodicity, which results from transesterification between the two polymers, favors the development of fringed micellar crystals that have larger values of l_c, rather than the development of normal chain-folded crystals.

Keywords : poly(ethylene terephthalate), polycarbonate, primary crystallization, secondary crystallization.

Introduction

Binary polymer blends may be made of pairs of polymers where one or both components are crystalline. For the blends with one crystallizable component (A), crystals of A may be dispersed in an amorphous phase. Alternatively, spherulites of A may grow in a matrix consisting primarily of the other component. One important consideration in this case is the location of the noncrystallizable component (B) in the microstructure. The B molecules may be included in interspherulitic regions, interfibrillar regions (i.e. between the lamellar stacks), interlamellar regions, or some combination of these.[1-4]

In addition to crystallization, morphologies of crystalline polymer blends may sometimes be influenced by a liquid-liquid (L-L) demixing process.[3,5-10] When the blend has a lower critical solution temperature (LCST) or upper critical solution temperature (UCST) phase diagram, crystallization may proceed simultaneously and compete with L-L phase separation. The competitive two processes may create unique morphological patterns that are not attainable by either process alone. In a recent study, we observed that an extruded poly(ethylene terephthalate) (PET)/polycarbonate (PC) blend exhibited combined crystallization and L-L demixing.[11] We carried out optical microscopy (OM) observations to confirm L-L phase separation via spinodal decomposition (SD), and investigated the effects of L-L demixing and subsequent phase homogenization on crystallization. The OM results showed that at the early stage of holding, L-L phase separation proceeded in the melt-extruded specimen. After the formation of domain structure, the blend slowly underwent phase homogenization by transesterification between the two polymers.

Although morphology development on the order of micrometers has been revealed for the PET/PC blend,[12,13] the microstructure of a finer scale still requires further exploration. In this article, we describe a study of the morphological changes in the PET/PC blend at a lamellar level. The morphological parameters, such as lamellar crystalline thickness (l_c) and amorphous layer thickness (l_a) were determined by small-angle X-ray scattering (SAXS) measurements. The characteristics of the structural development at lamellar levels are discussed on the basis of the effect of

*e-mail: polylee@inha.ac.kr

combined crystallization and L-L demixing.

Experimental

Materials. Commercial PET (M_w = 52,000, M_w/M_n = 2.0) produced by Honam Petrochemical Co.(Korea) was used. Bisphenol A polycarbonate (M_w = 36,000, M_w/M_n = 1.7) was obtained from Samyang Co.(Korea). After being dried in a vacuum oven at 150 °C for 24 hr, PET and PC were melt-mixed at 280 °C on a 30 mm corotating twin-screw extruder (Werner Pfleiderer) at 200 rpm. The residence time for the melt-mixing was less than 1 min. The extrudate was quenched in ice water to freeze the structure in the melt and was then chopped into pellets. The composition of the PET/PC blend was 50/50 by weight.

SAXS. SAXS was used to measure the isothermal crystallization of the PET/PC blend. The sample was melted at 280 °C for a certain time (t_s), and was then jumped to a desired crystallization temperature for measurement. The X-ray beam was from synchrotron radiation, beam line 4C1 at the Pohang Light Source (Korea). The storage ring was operated at an energy level of 2 GeV. SAXS employed point-focusing optics with a silicon double-crystal monochromator followed by a bent cylindrical mirror. The incident beam intensity with a wavelength of 0.149 nm was monitored by an ionization chamber for the correction of a minor decrease of the primary beam intensity during the measurement. The data collection time was 10 s per scattering frame.

The raw SAXS data were analyzed via the correlation function approaches.[14,15] The correlation function is the Fourier transform of the Lorentz-corrected SAXS data:

$$\gamma_1(r) = \frac{\int_0^\infty [I-I_b]q^2\cos(qr)dq}{\int_0^\infty [I-I_b]q^2dq} \quad (1)$$

where $\gamma_1(r)$ is the one-dimensional correlation function, I is the scattering intensity, I_b is the background intensity, and q is $(4\pi/\lambda)\sin(\theta/2)$, with λ and θ being the wavelength and scattering angle, respectively. Because SAXS data are collected in a limited angle range, it must necessarily be extrapolated to both high and low q values before Fourier transformation. The data were extrapolated to low q values (in the beam-stop region) under the assumption of a linear profile of $[I-I_b]\cdot q^2$ versus q^2. The extrapolation in the high q region was performed with the aid of Porod's law. Details of the Porod analysis are reported elsewhere.[16,17]

From the correlation function, we estimate L (the first maximum), l_c and l_a using the following equations[17,18]:

$$x_{cl}(1-x_{cl})L = B \quad (2)$$

$$x_{cl} = l_c/L \quad (3)$$

$$l_a = L-l_c \quad (4)$$

where $x_{cl} = l_c/L$ is the linear crystallinity within the lamellae structure and B is the position of the first intercept of the correlation function with the r axis. Note that eq. 2 is quadratic in x_{cl} and can be solved to obtain two solutions for x_{cl}. The sum of these two solutions will equal 1, and only one of these solutions corresponds to l_c. Wang *et al.*[18] studied in detail which one corresponds to l_c or l_a. They reported that the longer length deduced from the high value of x_{cl} is l_c and the shorter length given by L- l_c is l_a.

Results and Discussion

Phase Behavior. Previously, we reported the behavior of L-L phase separation and subsequent homogenization during holding in an extruded PET/PC blend.[11] Figure 1 shows optical micrographs of the PET/PC blend holding at 280 °C for t_s. In the beginning [Figure 1(a)], a high level of interconnectivity in both phases can be seen, and the phases are regularly spaced. At the later stage of L-L phase separation [Figure 1(b)], the phase connectivity grows and eventually breaks up into a macroscopic spherical texture. As the transesterification reaction proceeds, the domain growth is suppressed, and the blend morphology is mainly controlled by the phase homogenization process [Figure 1(c)]. Finally the blend shows a homogeneous mixture [Figure 1(d)]. Dynamic mechanical measurements provided supplementary evidence for the phase behavior. For the t_s = 3 min sample, two glass transition temperatures (T_g's) were shifted toward each other, suggesting that some level of phase separation existed. As t_s increased, the blend showed a single T_g. This indicated that the level of transesterification between the two polymers increased with t_s, leading to the formation of a single amorphous phase.

Lamellar Morphology. Figure 2 shows the plots of L, l_c, and l_a against t_s for the blend samples crystallized at 180 °C. The crystallization temperature of 180 °C was chosen based on our knowledge of the rapid growth rate of the PET crystals. Conceptually, it seems plausible that the rapid crystallization of PET at 180 °C is very effective to lock-in further growth of the L-L phase separation. The blend has a larger l_a than the pure PET (the l_a value of the pure PET sample crystallized at 180 °C was 35 Å[19]), suggesting that PC in the PET-rich phase is incorporated into the interlamellar regions during crystallization. It is seen that l_c of the blend is larger than the value of 58 Å for the pure PET.[19] This result might be explained simply by thermodynamic considerations. If the PC molecules act as a polymeric diluent for PET, the melting point of PET will be decreased. In that case, we would expect an increase in l_c at a given crystallization temperature because of the decrease in the degree of supercooling. However, the melting point depression of PET for the t_s = 1 min sample was a little over 1 °C (data not shown). Therefore, it seems that the other thermodynamic parameters are responsible for the increased l_c. In principle l_c could increase through the increase of quantity $(\sigma_e T_m^o)$[20]:

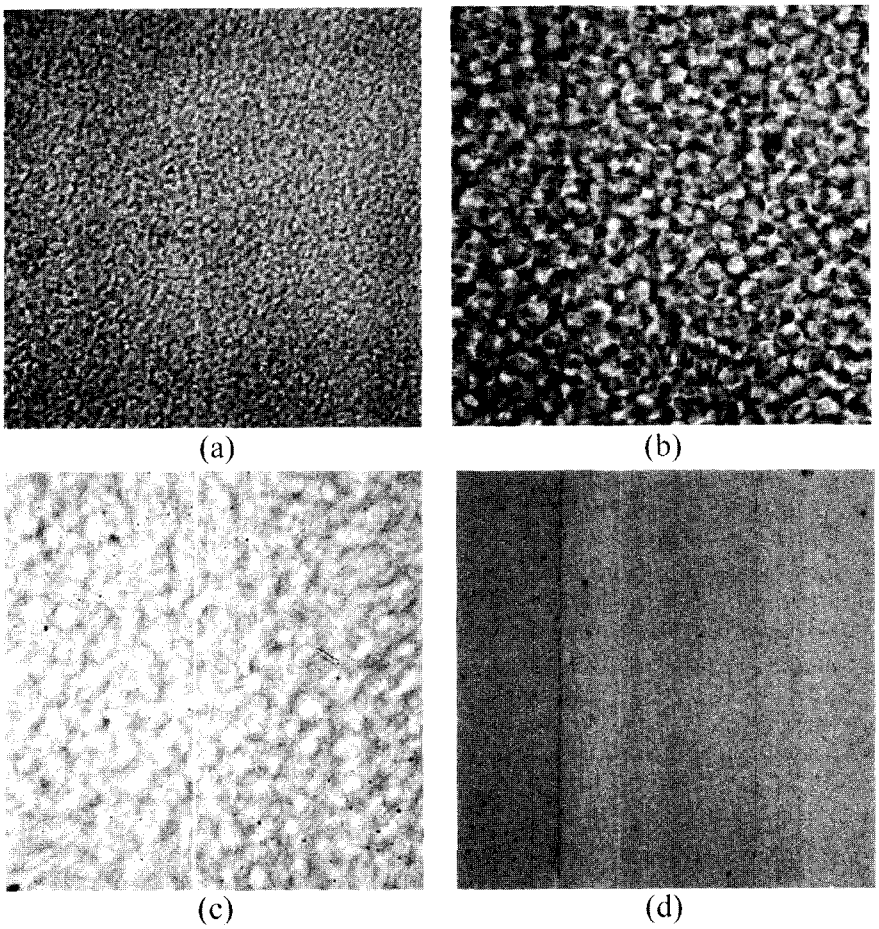

Figure 1. Optical micrographs of the PET/PC blend after holding at 280 °C for (a) t_s = 3 min, (b) t_s = 5 min, (c) t_s = 10 min, and (d) t_s = 15 min.

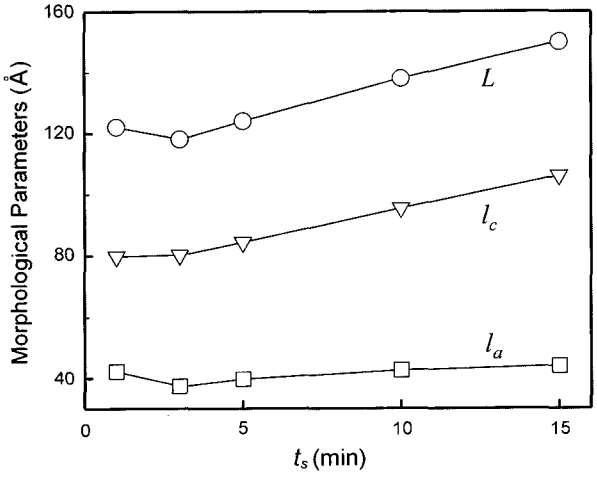

Figure 2. Plot of the lamellar dimensions (L, l_c, and l_a) against t_s for the PET/PC blend crystallized at 180 °C for 4 hr.

$$l_c = \frac{2\gamma\sigma_e T_m^o}{\Delta h_f \Delta T} \quad (5)$$

where γ is a constant, σ_e, the surface free energy of folding, T_m^o, the equilibrium melting temperature, Δh_f, the heat of fusion, and ΔT is the degree of supercooling. According to eq. (5), the increased l_c would suggest a strong influence of the PC molecules on σ_e. The inclusion of the PC molecules in the interlamellar regions during the growth of the PET crystals probably causes an increase of σ_e, leading to a larger value of l_c. However, our results do not seem to support such a hypothesis. One of interesting features in the figure is the change in l_a with t_s. l_a attains a minimum value at t_s = 3 min and then gradually increases. In the early stage of holding (t_s < 3 min; in this stage the blend morphology is mainly controlled by the L-L phase separation[11]), the PC molecules in a PET-rich phase may be forced to move to a PC-rich phase. As a result, the amount of PC in the PET-rich phase should decrease with t_s and the smaller amount of PC may be correspondingly incorporated into the interlamellar regions during crystallization. Therefore, it can be expected that the value of l_a for t_s = 3 min is lower than that for t_s = 1 min. However, the increase in l_a for t_s > 3 min may be attributed to the reduction in the crystallinity due to the transesterification

reaction (The crystallinity values of the t_s = 1, 3, 5, 10 and 15 min samples determined with DSC were 0.36, 0.35, 0.33, 0.30 and 0.27, respectively.). The increased PC component in the PET-rich phase by the phase homogenization may also contribute to the increasing value of l_a. It is worth noting that the PET crystals formed in PC-rich phase, which could have a larger value of l_a than those formed in PET-rich phase, may give an influence on the increase in l_a.

Figure 3 shows the time evolution of the SAXS invariant (Q) during isothermal crystallization at 180 °C. It can be seen that the curves for Q consist of two lines with abrupt change in the slope. The two regions of linear behavior are denoted regimes I and II: the regime I ($t < t_c$, t_c is the intersection of the two lines) and regime II are characterized by the primary crystallization process and the secondary crystallization process, respectively.[4] The value of Q for the t_s = 3 min sample reaches a plateau when the primary crystallization is complete. With increasing t_s, the secondary crystallization process becomes important, and a relatively large fraction of crystallinity develops after the primary crystallization. Secondary crystals naturally form in topologically restricted regions, probably in the gaps between primary lamellar stacks. Recently, the growth of secondary stacks of lamellae was physically justified and also modeled.[21] According to the model, the entire primary stacks or fibrils grow radially in a way that the spherulite is not fully dense, leaving gaps of various dimensions for the secondary lamellar stacks. Because of the low molar-mass species, impurities, and lower entropy restraints in the amorphous regions restrained by the primary crystals, it is believed that the secondary crystals possess a thinner lamellar thickness and defective crystal structure. Therefore, the secondary crystallization may be accompanied with a distinct change in the crystalline structure at both the spherulitic and lamellar levels if the contribution of the primary and secondary crystallization processes to the development of the overall crystallinity is comparable.

The spherulitic morphology of the blend was investigated with small-angle light scattering. Figure 4 shows H_v scattering patterns for the samples holding for t_s = 3 and 15 min and subsequently crystallized isothermally at 180 °C. A typical four-leaf clover pattern is observed for the t_s = 3 min sample. The pattern with lobes at 45° to the polarization direction has been interpreted as arising from optic axes oriented parallel or perpendicular to the spherulite radius. With increasing t_s, the pattern becomes diffuse and less azimuthally dependent. The H_v scattering pattern is concerned with the arrangement of the individual lamellar crystallites into a lager scale of organization. Stein and Chu[22] suggested by the model calculation of the scattering patterns that lower orders of organization result in the broad H_v scattering pattern, i.e. as the disorder of lamellar orientation increases, the azimuthal dependence of the scattering pattern becomes less and the scattering pattern shows a diffuse pattern. The orientation

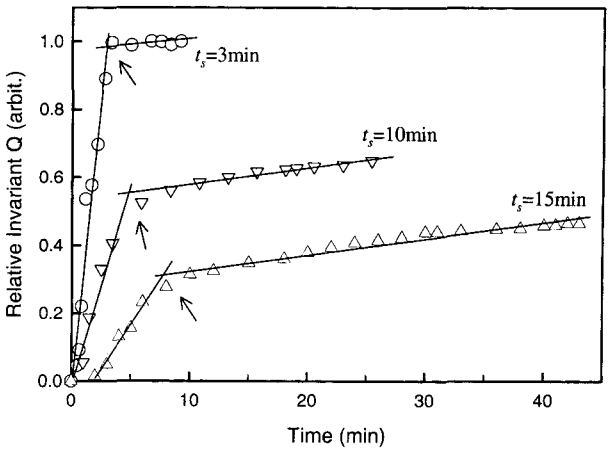

Figure 3. Time variation of the SAXS invariant Q for the PET/PC blend crystallized at 180 °C after holding at 280 °C for t_s.

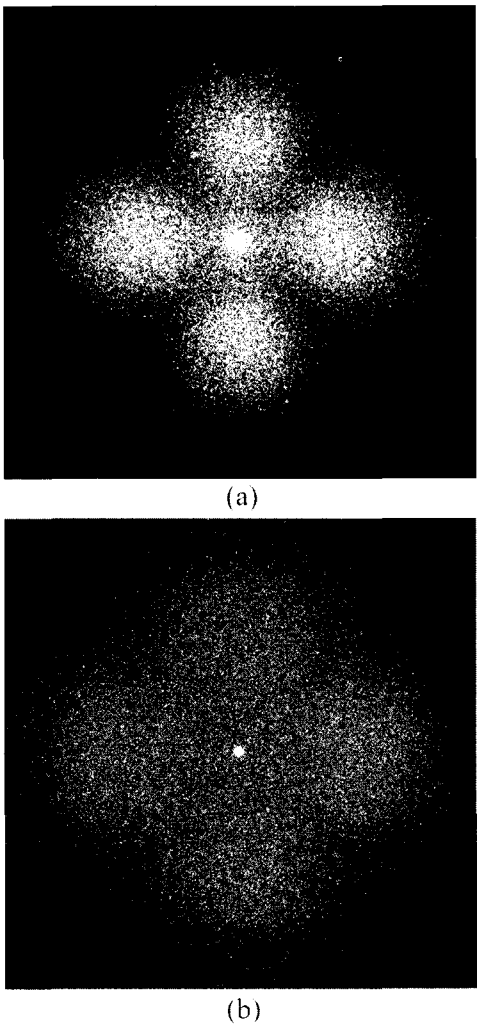

Figure 4. H_v light scattering patterns for the PET/PC blend crystallized at 180 °C for 4 hr after holding at 280 °C for (a) t_s = 3 min, and (b) t_s = 15 min.

fluctuation of the lamellar crystals within a spherulite can be quantitatively described by introducing the disorder parameter ξ. Yoon and Stein[23] provided a calibration curve relating the parameter ξ to the ratio of intensity at $w = 4$ to that at $w = 15$, where w is the reduced angle parameter defined as:

$$w = (2\pi/\lambda)\, R \sin\theta \tag{6}$$

$$\xi = I(w = 4) / I(w = 15) \tag{7}$$

where R is the radius of spherulite. As ξ increases, the peak intensity at a scattering angle θ_m decreases and the intensity decreases more gradually with θ. The calculated value of ξ for the $t_s = 15$ min sample was 0.21, which was much larger than the value of 0.07 for the $t_s = 3$ min sample. While we cannot examine our experimental data in a more quantitative or theoretical method, some general remarks can be made. Because the chain constitution gives a large influence on the supermolecular structure,[24,25] the incorporation of copolymer units or other irregularities into the chain may alter the major characteristics of the spherulitic morphology. Thus, it can be inferred that the increase of the sequence distribution in polymer chains via transesterification restricts the formation of well-ordered spherulites and favors randomly arranged lamellae.

To follow the development of lamellar morphology during crystallization, the variation of parameters such as L, l_c, and l_a has been extracted from the time-resolved SAXS data. The data in Figure 5 show rapid decreases in l_c during the primary crystallization, which is consistent with many experimental observations in the literature,[4,26-29] but with few explanations provided. It can be explained by defective lamellar stacks filling in the space of spherulites, as the secondary crystals form in the nominal primary crystallization regime.[4] It is noted that the values of l_a remain approximately constant during prolonged times; we thus believe that the formation of secondary lamellae in the PET/PC blend system may mainly occur between the primary stacks rather than within the primary stacks. A unique observation in the figure is that the value of l_c for the $t_s = 15$ min sample is seen to significantly increase during the secondary crystallization. Since the secondary crystallization normally produces thinner lamellar stacks with smaller values of l_c, this trend may appear contradictory. As mentioned previously, the interchange reactions between the two polymers give rise to the disruption of chain periodicity. If the crystallizable sequence lengths of the PET-PC copolymers are too short to participate in lamellar growth by a chain folding mechanism, the secondary crystallization may only occur through clustering of chain segments and lead to the formation of fringed micellar crystals. Here, the term fringed micellar crystal is representative of an aggregate of chains exhibiting some

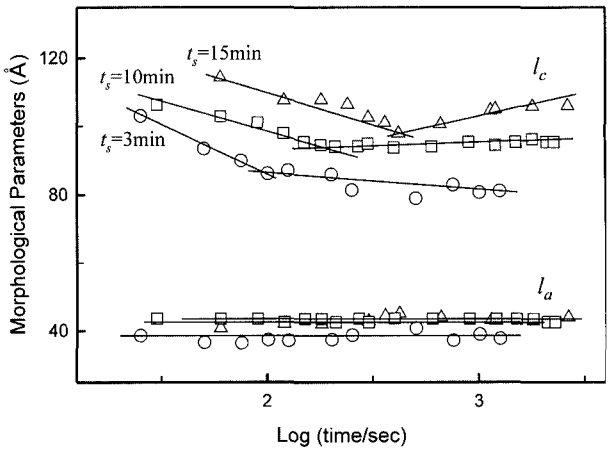

Figure 5. Time variation of the morphological parameters (l_c and l_a) for the PET/PC blend crystallized at 180 °C after holding at 280 °C for t_s.

level of crystallographic packing over restricted distances in directions parallel and normal to the chain axis or an chain cluster which forms from shorter sequences.[30] The fraction of the micellar crystals will be probably enhanced with t_s because of the increased level of transesterification. Therefore, it is likely that the lamellar thickening in the secondary crystallization dominant regime may be attributed to the unusual secondary crystallization process which favors the development of fringed micellar crystals with larger values of l_c. However, more experimentals, e.g. transmission electron microscopy (TEM), will be needed to clarify our speculation.

Conclusions

We studied the morphological changes at the lamellar level in the PET/PC blend. On the basis of the results described in this article, we were able to make the following conclusions: (1) A rapid decrease in l_c at early crystallization times suggested that the growth of secondary stacks of lamellae would also proceed in the nominal primary crystallization regime; (2) A constant value of l_a during the overall crystallization implied that the secondary crystals might form between the existing primary lamellar stacks; (3) A large disruption of chain periodicity as a consequence of transesterification would favor the development of fringed micellar crystals rather than that of normal chain-folded crystals, leading to the lamellar thickening during the secondary crystallization.

Acknowledgements. This research was supported by the Center for Advanced Functional Polymers. Synchrotron SAXS experiments were performed at the Pohang Light Source (4C1 beam line) in Korea, which was supported by MOST and Pohang Iron & Steel Co. (POSCO).

References

(1) S. Talibuddin, L. Wu, J. Runt, and J. S. Lin, *Macromolecules*, **29**, 7527 (1996).
(2) H. L. Chen, L. J. Li, and T. L. Lin, *Macromolecules*, **31**, 2255 (1998).
(3) H. L. Chen and M. S. Hsiao, *Macromolecules*, **31**, 6579 (1998).
(4) F. Yeh, B. S. Hsiao, B. Chu, B. B. Sauer, and E. A. Flexman, *J. Polym. Sci., Polym. Phys. Ed.*, **37**, 3115 (1999).
(5) N. Inaba, K. Sato, S. Suzuki, and T. Hashimoto, *Macromolecules*, **19**, 1690 (1986).
(6) N. Inaba, T. Yamada, S. Suzuki, and T. Hashimoto, *Macromolecules*, **21**, 407 (1988).
(7) H. L. Chen, J. C. Hwang, J. M. Yang, and R. C. Wang, *Polymer*, **39**, 6983 (1998).
(8) S. Nojima, K. Sato, and T. Ashida, *Macromolecules*, **24**, 942 (1991).
(9) M. Okamoto and T. Kotaka, *Polymer*, **38**, 1357(1997).
(10) H. J. Bang, J. K. Lee, and K. H. Lee, *J. Polym. Sci., Polym. Phys. Ed.*, **38**, 2625 (2000).
(11) J. K. Lee, J. E. Im, and K. H. Lee, *Euro. Polym. J.*, submitted (2003).
(12) M. Garcia, J. I. Eguiazabal, and J. Nazabal, *J. Appl. Polym. Sci.*, **81**, 121 (2001).
(13) Y. Kong and J. N. Hay, *Polymer*, **43**, 1805 (2002).
(14) S. Buchner, D. Wiswe, and H. G. Zachmann, *Polymer*, **30**, 480 (1989).
(15) G. R. Strobl and M. Schneider, *J. Polym. Sci., Polym. Phys. Ed.*, **18**, 1343 (1980).
(16) R. K. Verma, V. Velikov, R. G. Kander, H. Marand, B. Chu, and B. S. Hsiao, *Polymer*, **37**, 5357 (1996).
(17) R. Verma, H. Marand, and B. Hsiao, *Macromolecules*, **29**, 7767 (1996).
(18) W. Wang, J. M. Schultz, and B. S. Hsiao, *Macromolecules*, **30**, 4544 (1997).
(19) J. K. Lee, H. J. Bang, and K. H. Lee, *J. Polym. Sci., Polym. Phys. Ed.*, **40**, 317 (2002).
(20) E. Martuscelli, *Polym. Eng. Sci.*, **24**, 563 (1984).
(21) B. S. Hsiao, I. Y. Chang, and B. B. Sauer, *Polymer*, **32**, 27 (1991).
(22) R. S. Stein and W. J. Chu, *Polym. Sci. A-2*, **8**, 1137 (1970).
(23) D. Y. Yoon and R. S. Stein, *J. Polym. Sci., Polym. Phys. Ed.*, **12**, 763 (1974).
(24) A. Lilaonitkul, J. C. West, and S. L. Cooper, *J. Macromol. Sci. Phys. B*, **12**, 563 (1976).
(25) M. Matsuo, K. Geshi, A. Moriyama, and C. Sawatari, *Macromolecules*, **15**, 193 (1982).
(26) G. Elsner, H. G. Zachmann, and J. R. Milch, *Makromol. Chem.*, **182**, 657 (1981).
(27) A. M. Jonas, T. P. Russell, and D. Y. Yoon, *Macromolecules*, **28**, 8491 (1993).
(28) K. N. Kruger and H. G. Zachmann, *Macromolecules*, **26**, 5202 (1993).
(29) R. A. Phillips, Z. G. Wang, and B. S. Hsiao, *ACS PMSE Proc.*, **79**, 295 (1998).
(30) A. Alizadeh, L. Richardson, J. Xu, S. McCartney, H. Marand, Y. W. Cheung, and S. Chum, *Macromolecules*, **32**, 6221 (1999).